Electroplastic Behavior of Doped Poly(3-hexylthiophene)

TOHRU SHIGA* and AKANE OKADA

Toyota Central Research and Development Laboratories Inc., Nagakute-cho, Aichi-gun, Aichi-ken, 480-11, Japan

SYNOPSIS

Dynamic viscoelasticity of poly(3-hexylthiophene) (P3HT) doped with iodine or $FeCl_3$ under the influence of electric fields was studied. The doped P3HTs underwent a large decrease in elastic modulus under small electric fields on the order of 1 dc V/mm. The electric fields enhanced the loss tangent. The glass transition temperature decreased as the intensity of the applied fields was increased. This electroplastic behavior was observed also in ac excitation of less than 1 kHz. It was detected in both crystalline and amorphous P3HTs. Joule heating was a main process in the electroplastic behavior of doped P3HTs. We measured FTIR and X-ray diffraction spectra under electric fields to examine the possibility of other processes. The X-ray diffraction analysis suggested a possibility of another process caused by the formation of intra-planar packing of thiophene rings. © 1996 John Wiley & Sons, Inc.

INTRODUCTION

The structure of complex fluids can be dramatically affected by applied electric and magnetic fields. Electrorheological (ER) fluids are colloidal suspensions in which applied electric fields both alter the structure of the fluids and strongly influence its apparent viscosity.[1-5] Magnetorheological (MR) fluids display similar phenomena in magnetic fields.[6,7] Such rheological behaviors, known as ER or MR effects, are caused by alignments of electromagnetically polarized particles between electrodes. Recently, the ER or MR effects have been detected also in polymer gels. A composite of silicone gel and poly(methacrylic acid) cobalt (II) particles enhanced its elastic modulus by action of electric fields on the order of 1 kV/mm.[8,9] It was found that a magnetic field of 50 kA/m hardened a silicone gel containing iron particles.[10] The ER and MR effects in polymer gels offer the possibility of electromagnetic control of the viscoelasticity of an immiscible polymer blend.

In previous articles,[11,12] we investigated the viscoelastic behavior of the particulate composites of conducting polymer particles in electric fields. The composite gels of lightly doped poly(*p*-phenylene) particles stiffened in electric fields, as we had expected. It was, however, found that silicone gels containing iodine-doped poly(3-hexylthiophene) (P3HT) particles softened under electric fields. Since it was suggested that the electroplastic behavior of the iodine-doped P3HT particle system was caused by the softness of the P3HT particles, we directly measured the dynamic viscoelasticity of P3HT doped with iodine or $FeCl_3$ under an electric field. Here, we report that doped P3HTs in an electric field show a large decrease in the elastic modulus or the glass transition temperature. We also discuss the mechanism of the electroplastic behavior of doped P3HTs.

EXPERIMENTAL

Preparation of P3HT

The starting monomer, 3-hexylthiophene (3HT), was synthesized via the coupling of hexylmagnesium bromide with 3-bromo-thiophene in the presence of $Ni(dppp)Cl_2$ according to the method of Tamao et al.[13] P3HT was prepared by electrochemical polymerization or by oxidative coupling of 3HT. The electrochemical polymerization was carried out with $(C_4H_9)_4\ NBF_4$ in nitrobenzene.[14] The undoping of BF_4^- was achieved by exposing the prepared polymer

* To whom correspondence should be addressed.

Journal of Applied Polymer Science, Vol. 62, 903-910 (1996)
 CCC 0021-8995/96/060903-08

Table I DC Conductivity of Samples

No.	Polymer	Dopant	[Dopant] (Wt %)	σ (S/cm)
1	Crystalline	Undoped	0	3.61×10^{-9}
2	Crystalline	$FeCl_3$	1.90	4.67×10^{-1}
3	Crystalline	$FeCl_3$	4.41	8.31×10^{-1}
4	Crystalline	$FeCl_3$	7.25	6.25×10^{-1}
5	Crystalline	Iodine	13.8	2.45×10^{-1}
6	Crystalline	Iodine	23.2	8.89×10^{-1}
7	Crystalline	Iodine	31.8	7.18×10^{-1}
8	Amorphous	Undoped	0	$<1 \times 10^{-9}$
9	Amorphous	$FeCl_3$	6.27	2.18×10^{0}
10	Amorphous	Iodine	21.7	1.67×10^{0}

to a reversed electric field in fresh nitrobenzene. The oxidative coupling was made using $FeCl_3$ in chloroform.[15] The prepared polymer was washed several times with 2*N* HCl at 70°C. The P3HTs obtained from the two methods were dissolved in chloroform. After filtration of insoluble P3HT gel, the solvent was evaporated to give P3HT cast films (thickness 110 μm). According to our X-ray diffraction analysis, the P3HT film by oxidative coupling was crystalline while the film by electrochemical polymerization was amorphous (see Figs. 9 and 10). Here, we call the two P3HTs crystalline P3HT and amorphous P3HT, respectively. When calibrated against polystyrene standards, values of the molecular weight of the P3HTs, $M_w = 54{,}300$, $M_w/M_n = 2.51$ (crystalline P3HT) and $M_w = 55{,}400$, $M_w/M_n = 1.79$ (amorphous P3HT) were obtained.

Doping

Chemical doping was carried out by exposing the P3HT film to a vapor of iodine at 80°C for 5 h or by immersing that in a $FeCl_3$–nitromethane solution of 0.1 mol/L at room temperature for several minutes.[16] The content of the dopants was calculated using weights of undoped and doped P3HT films. The dopant content and dc conductivity of the P3HT films as samples are listed in Table I. Dc conductivity was calculated using the equation $\sigma = IS/Vd$ (*I*, electrical current; *V*, applied voltage; *S*, area of cross section of sample; and *d*, gap between electrodes; see Fig. 1).

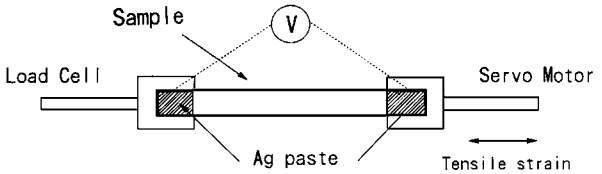

Figure 1 Schematic illustration of a test apparatus for viscoelastic measurement under electric fields.

Measurement of Viscoelasticity

The experiments were performed in air on a viscoelastic spectrometer (Iwamoto Seisakuzyo Ltd. VES-F). Figure 1 indicates a schematic illustration of a test apparatus for viscoelastic measurement. Both ends of the sample were coated with Ag paste (Fuzikura Kasei Ltd., Dotite D-550) as electrodes. The test apparatus was set in a chamber of the viscoelastic spectrometer and then dc voltages up to 200 V or ac voltages between 0.1 Hz and 1 kHz were applied between the Ag electrodes. The sample was vibrated at a sinusoidally varying tensile strain, $\varepsilon = 0.1 \sin(2\pi ft)$, by a servomotor. The frequency of the applied strain *f* was between 0.1 and 100 Hz. Torque acting on the sample was measured in the temperature range from −50 to 50°C through the load cell. Storage and loss moduli, E' and E'', and loss tangent tan δ of the samples were calculated automatically by a personal computer. The temperature dependencies of the mechanical parameters were measured by heating the chamber at a rate of 2°C/min.

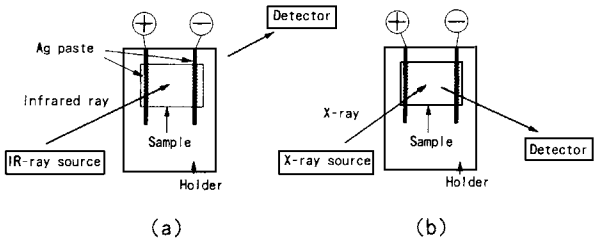

Figure 2 Schematic illustrations of (a) FTIR and (b) X-ray diffraction measurements under electric fields.

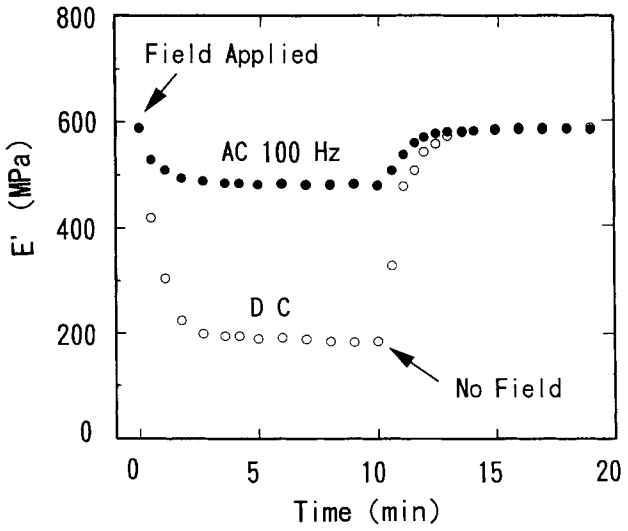

Figure 3 Temporal changes in storage modulus in electric fields. The sample used was no. 6 in Table I. The applied fields were 0.44 dc V/mm and a 100 Hz field of 0.44 V/mm. In Figures 3–5, the experiments were carried out at room temperature using a strain frequency of 10 Hz.

Measurement of FTIR Spectra

To investigate a change in chemical structure due to electric fields, FTIR spectra of the samples in electric fields were measured at room temperature [Fig. 2(a)]. The experiments were performed on an FTIR spectrometer (Nippon Bunkou, FTIR/5M) using P3HT films with a thickness of ca. 5 μm.

Measurement of X-ray Diffraction Spectra

X-ray diffraction patterns under electric fields were measured to examine the possibility of a change in the physical structure of P3HT chains in the electric fields [Fig. 2(b)]. The experiments were carried out at room temperature in a 2θ range between 3° and 60° using a Rigaku X-ray diffractometer (RAD-2B). The X-ray source utilized a copper target (λ = 1.541 Å).

RESULTS AND DISCUSSION

Viscoelasticity in Electric Fields

The doped P3HTs changed in mechanical properties when subjected to electric fields on the order of 1 V/mm. Figure 3 indicates storage modulus–time curves of iodine-doped P3HT (no. 6 in Table I) in dc or ac electric fields. E' decreases by the action of a dc electric field and reaches a constant value in about 3 min. We call this phenomenon the electroplastic effect. When the applied field is removed, the parameter recovers the starting value in the absence of an electric field. The response speed upon the applied field is almost equal to the reversing speed. As shown in Figure 3, the electroplastic effect has been detected in ac excitation of 100 Hz. It does, however, disappear in ac fields of more than 1 kHz. It suggests that ionic polarization is strongly associated with the electroplastic effect. It is found that dc excitation gives a large electroplastic effect. The difference between ac and dc fields may probably be due to the current distribution in the sample. We next examined the relationship between electric

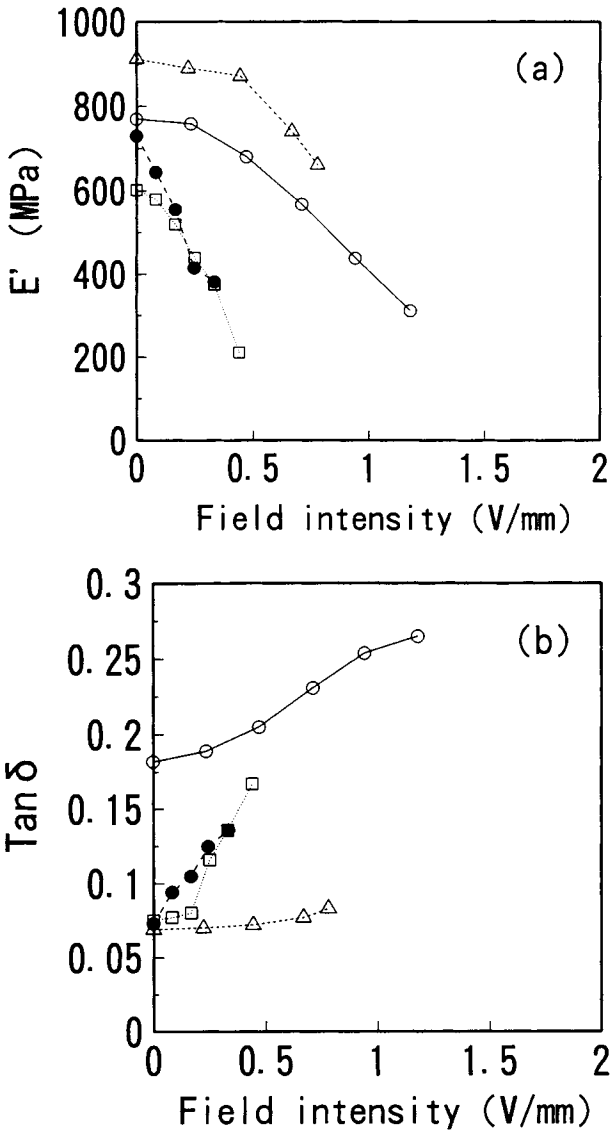

Figure 4 (a) Storage modulus E' and (b) loss tangent tan δ of doped P3HTs under various dc electric fields. Samples: (○) no. 3; (△) no. 4; (□) no. 6; (●) no. 10.

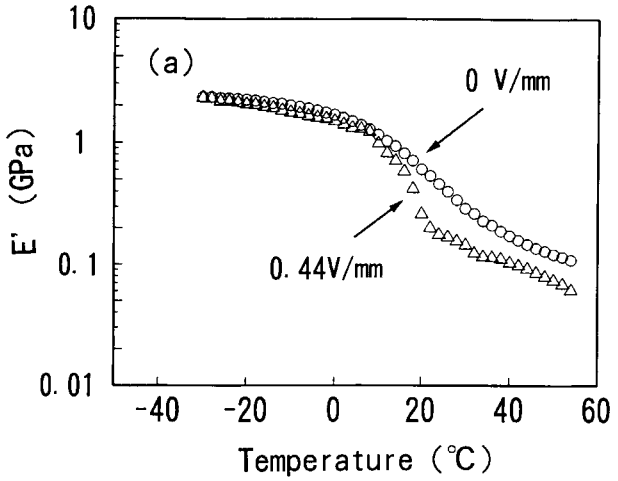

Figure 5 Temperature dependencies of E' with and without electric fields: (○) 0 V/mm; (△) 0.44 dc V/mm. The horizontal axis represents the temperature in a test chamber of the viscoelastic spectrometer.

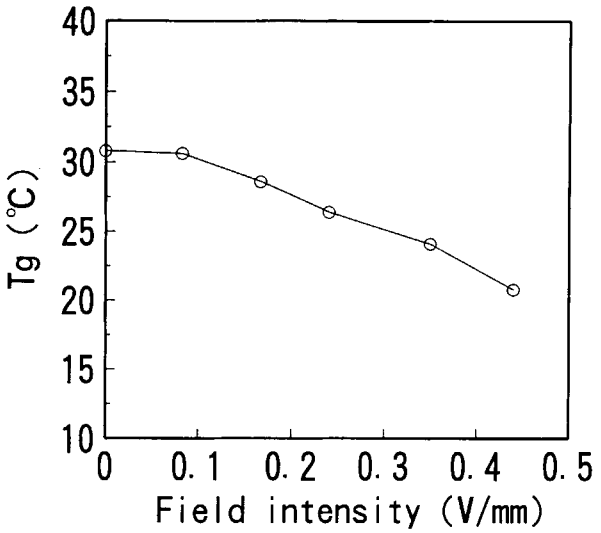

Figure 6 Glass transition temperature of doped P3HT under various electric fields. The sample used was no. 3.

power input to the samples and the magnitude of the electroplastic effect. The decrease in E' induced by electric fields was proportional to the electric power.

Figure 4(a) and (b) indicates the viscoelasticity of doped P3HTs under various dc electric fields. The values of E' and of tan δ after 3 min of the exposure time to electric fields are plotted as functions of the intensity of the applied fields. E' decreases with the intensity of the applied fields on the order of 1 V/mm. The crystalline P3HT [no. 3 (○)] shows a large decrease of 465 MPa under an electric field of 1.22 V/mm. On the other hand, tan δ increases in electric fields. The field of 1.22 V/mm induces an increase of 0.09 in tan δ (the value of δ changes from 10.2° to 15.0°). The electroplastic effect was observed also in amorphous P3HTs [no. 10 (●)].

In Figure 5 are displayed temperature dependencies of E' with and without an electric field. The electroplastic effect is not practically observed in the glassy state of P3HT. It affects the glass transition temperature T_g. As shown in Figure 6, T_g decreases gradually as the intensity of the applied field is increased. An electric field of 0.44 V/mm leads to a diminution of 10°C. The results obtained in Figures 4–6 suggest that the rigidity and damping property of the doped P3HTs can be controlled by electric signals.

Influence of Joule Heating on the Electroplastic Effect

Since the doped P3HTs have dc conductivities on the order of 10^{-1} S/cm, an electric current is carried in the sample under the applied fields. If Joule heating due to the electric current warms the sample, that may lead to a decrease in elastic modulus. To understand the mechanism of the electroplastic effect, we first estimated the influence of Joule heating on the electroplastic effect. The estimation was carried out as follows: A temperature increase at the surface of the sample in electric fields was measured directly using a thermometer (Tsuruga Ltd., Model 13527). There may be no difference in temperature between the inside and the surface of the sample because the samples are thin films (thickness 110 μm). Second, a decrease in E' ($\Delta E'_1$) due to the tem-

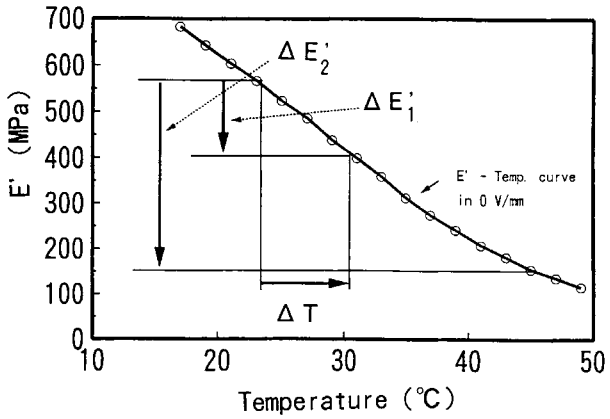

Figure 7 Estimation of a decrease of E' induced by Joule heating. ΔT is a temperature increase at the surface of sample induced by electric fields. $\Delta E'_1$ and $\Delta E'_2$ represent decreases of E' due to Joule heating and by electric fields, respectively.

Table II Influence of Joule Heating on the Electroplastic Effect

No.	Field (V/mm)	ΔT (°C)[a]	$\Delta E'_1$ (MPa)[b]	$\Delta E'_2$ (MPa)[c]	$\Delta E'_1/\Delta E'_2$ (%)
2	2.00	4.5	17	36	47.2
3	1.21	10.1	242	467	51.8
4	0.82	13.8	128	243	52.7
6	0.33	14.6	125	204	61.3
7	0.40	12.1	230	413	55.7
9	0.32	20.2	204	387	52.7
10	0.32	17.2	196	354	55.4

[a] Temperature increase by electric fields.
[b] Decrease of E' due to Joule heating.
[c] Decrease of E' by electric fields.

perature increase, indicating a decrease in E' by Joule heating, was calculated using an E'–temperature curve in the absence of an electric field [see symbol (○) in Fig. 7]. We finally compared $\Delta E'_1$ with a decrease in E' ($\Delta E'_2$) observed in the electric fields. The ratio of $\Delta E'_1$ to $\Delta E'_2$ represents the fraction of Joule heating on the electroplastic effect. The results are summarized in Table II. The ratios of $\Delta E'_1$ to $\Delta E'_2$ are between 50 and 60%. Table II indicates that Joule heating is the main process influencing the electroplastic effect of the doped P3HTs. The electroplastic effect is not, however, based simply on the Joule heating effect. The results obtained show a possibility of other processes.

FTIR Spectra in Electric Fields

FTIR spectra of the samples in electric fields were measured to investigate whether a change in chemical structure occurred in the electric fields [Fig. 8(a) and (b)]. FTIR spectra A and B represent undoped P3HT (no. 1 in Table I) and $FeCl_3$-doped P3HT (no. 2) in no field, respectively. They are the same as reported by Wang and Rubner.[17] Spectrum C exhibits $FeCl_3$-doped P3HT (no. 2) under 2 V/mm. The influence of the electric fields on the iodine-doped P3HT (no. 5) is shown in spectra D and E in Figure 8(b). No difference was found in the FTIR spectra with and without electric fields. These results say that the chemical structure of P3HT is unchanged in the applied electric fields.

X-ray Diffraction in Electric Fields

X-ray diffraction measurements were made to investigate a change in the physical structure of P3HT chains induced by the electric fields. X-ray diffraction patterns in the electric fields are displayed in Figures 9 and 10. In spectrum A of undoped crystalline P3HT (no. 1) in Figure 9(a), the three low-angle peaks at $2\theta = 5.09°$, 10.53°, and 15.91° correspond to first-, second-, and third-order reflections from the interlayer spacing, respectively.[18–20] When doping with $FeCl_3$ or iodine is done, the peak positions are shifted to lower angles (spectra B and D). Those are indicative of the expansion of interlayer spacing. Winokur et al. reported the same expansion of the interlayer spacing for poly(3-octylthiophene) or poly(3-dodecylthiophene) moderately doped with iodine.[21] When a dc electric field is applied, the expansion of the interlayer spacing is induced (spectra C and E). In the presence of an electric field, a new peak was detected at $2\theta = 23$–24° (see arrow points in spectra C and E). When the applied field was removed, the new X-ray peak disappeared in a few minutes. So, the occurrence of the new peak may be caused by dc electric fields.

Figure 10(a) and (b) indicates X-ray diffraction patterns of amorphous doped P3HTs. In spectrum C of iodine-doped P3HT, two new peaks appear at $2\theta = 14.5°$ and $2\theta = 23.4°$ under the influence of the electric fields. On the other hand, the X-ray diffraction pattern of $FeCl_3$-doped P3HT is unchanged by the action of the electric fields (spectra D and E).

From the results in Figures 9 and 10, it is found that X-ray diffraction patterns vary in the electric fields. To investigate the effect of Joule heating on the change in X-ray diffraction, we next measured X-ray diffraction patterns of $FeCl_3$-doped P3HT at 23 and 40°C in the absence of the electric fields (Fig. 11). The temperature of 40°C was determined by measuring the temperature at the surface of the sample under the applied electric field. At 40°C, the peaks of the first, second, and third diffractions shift to the lower-angle side. The intensity of the third-order diffraction increases in the electric field.

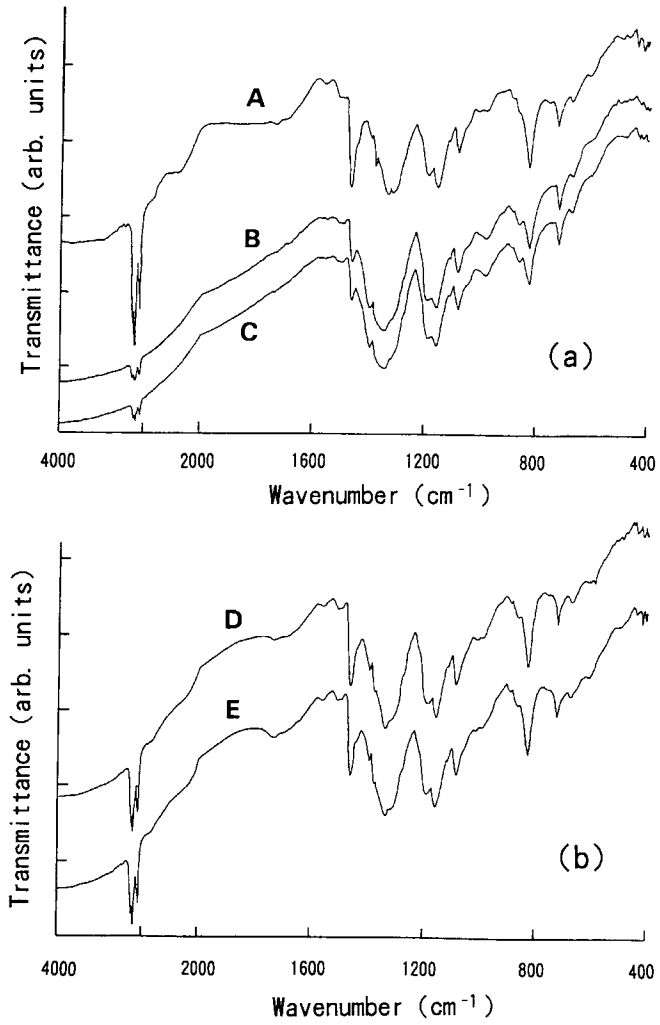

Figure 8 FTIR spectra of (a) $FeCl_3$-doped P3HTs and (b) iodine-doped P3HTs in electric fields. Spectra: (A) no. 1 (0 V/mm); (B) no. 2 (0 V/mm); (C) no. 2 (2 V/mm); (D) no. 5 (0 V/mm); (E) no. 5 (0.33 V/mm).

Therefore, the changes at low angles observed in the electric fields may be caused by Joule heating. On the other hand, there is no peak at a wide angle at 40°C. So, it is reasonable that the peaks at a wide angle shown in Figures 9(a) and (b) and 10(a) may be induced by electric fields rather than by Joule heating.

There are two explanations for the electric field-induced peak at a wide angle. One is a conformational change in P3HT chains. Chen and Ni proposed that the peak at $2\theta = 23.8°$ (d-spacing: 3.8 Å) could be attributed to the intralayer spacing between two successive stacking planes of co-planar subchains (intraplanar packing).[19] In our study, the electric field may cause the formation of intraplanar packing. Since it may probably bring about a dim-

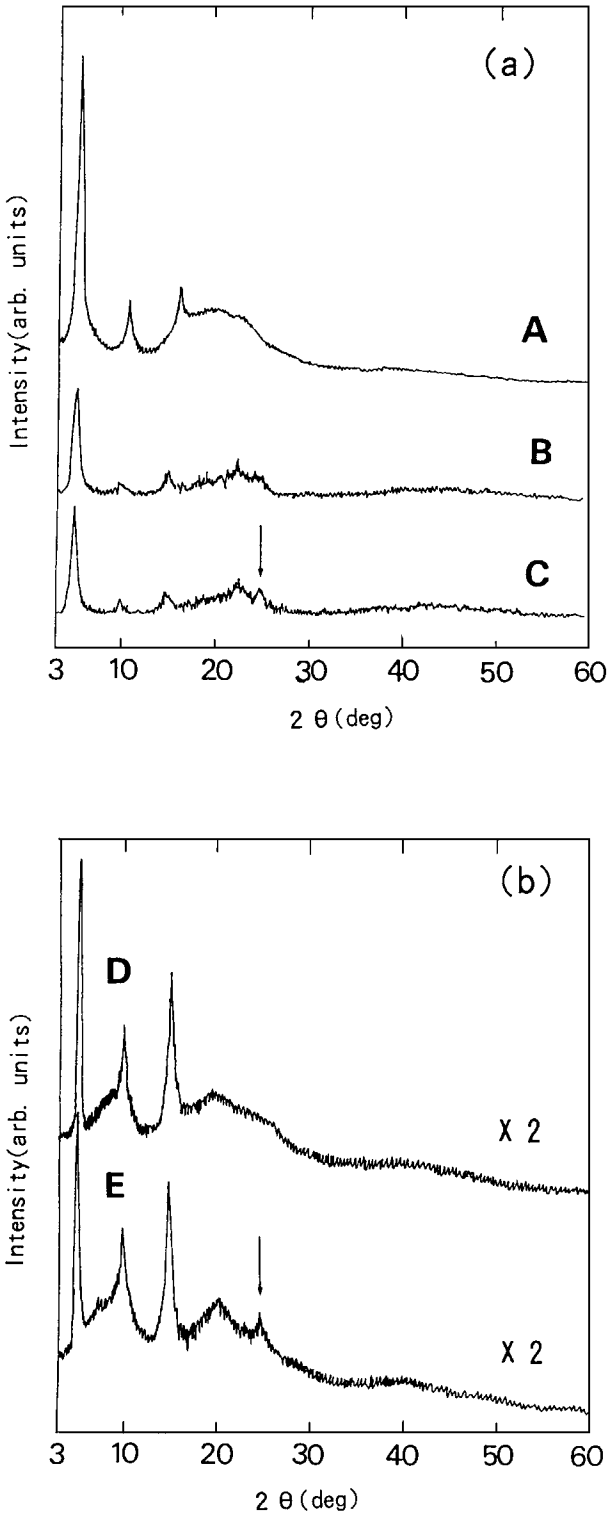

Figure 9 X-ray diffraction patterns of crystalline P3HTs doped (a) with $FeCl_3$ and (b) with iodine. Patterns: (A) no. 1 (0 V/mm); (B) no. 3 (0 V/mm); (C) no. 3 (1 V/mm); (D) no. 6 (0 V/mm); (E) no. 6 (0.33 V/mm). In Figures 9 and 10, the notation $\times n$ represents a magnification of intensity.

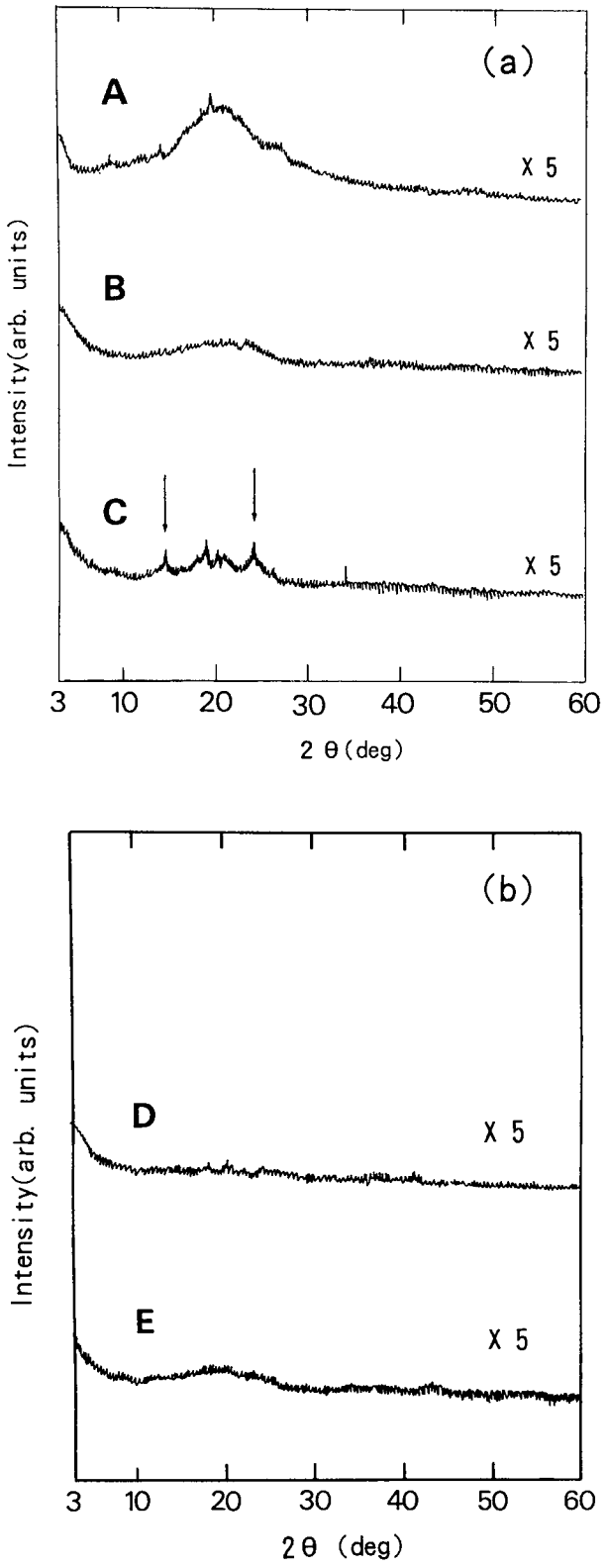

Figure 10 X-ray diffraction patterns of amorphous P3HTs doped (a) with iodine and (b) $FeCl_3$. Patterns: (A) no. 8 (0 V/mm); (B) no. 10 (0 V/mm); (C) no. 10 (0.5 V/mm); (D) no. 9 (0 V/mm); (E) no. 9 (0.33 V/mm).

inution of an interaction between the interlayers, the intralayer packing will lead to a decrease in the elastic modulus. The other explanation is that the undoping process proceeds in electric fields. It is well known that undoping induces a volumetric change of the conducting polymer and a decrease in E'.[22] Although undoping is not induced practically by an electric field, the interaction between polymer chains and dopants may weaken in electric fields. As shown in Figures 9(a), (b), and 10(a), the peaks observed at 2θ = 23–24° in the electric fields are clear and sharp. They look like signals from crystalline polymer. If the interaction between polymer chains and dopants weakens in the electric fields, the X-ray diffraction pattern at wide angles may become broad, like patterns A in Figures 9(a) and 10(a). It is, therefore, maintained that the former explanation may be correct.

CONCLUSION

The electroplastic effect of doped P3HTs which we have identified is a unique phenomenon and will have a great impact in conducting polymer technologies. The favorable feature of the electroplastic effect is that a large decrease in the elastic modulus on the order of 500 MPa is induced by the action of small electric fields on the order of 1 V/mm. The doped P3HT shows a better electromechanical effect than do the ER or MR gels.[8-10] Although the mechanism of the electroplastic effect was not analyzed

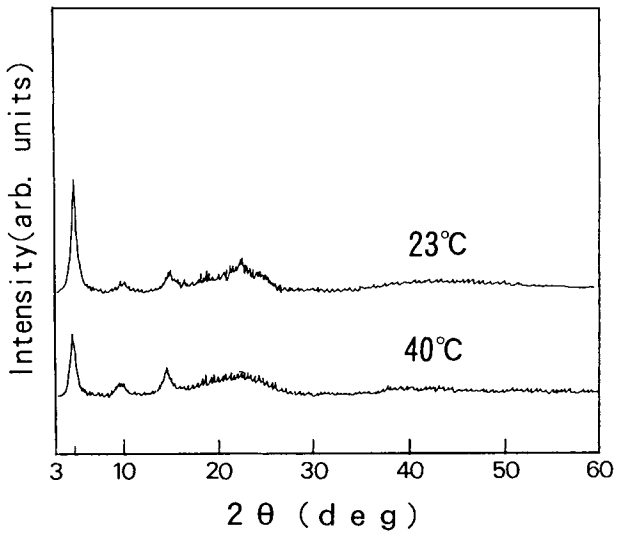

Figure 11 X-ray diffraction patterns of $FeCl_3$-doped P3HT at 23 and at 40°C in no electric field. The sample used was no. 3.

perfectly, it was found that the electroplastic effect could not be explained simply by Joule heating. The X-ray diffraction studies suggested the possibility of another process which was based upon the formation of the intraplanar packing of the thiophene rings.

REFERENCES

1. W. M. Winslow, U.S. Pat. 2,417,850 (1947).
2. J. E. Stangroom, *Phys. Technol.*, **14,** 290 (1983).
3. D. L. Klass, and T. W. Martinek, *J. Appl. Phys.*, **38,** 75 (1967).
4. D. J. Klingenberg, F. van Swol, and F. J. Zukoski, *J. Chem. Phys.*, **91,** 7888 (1989).
5. H. Block and J. P. Kelly, *Spec. Publ. R. Soc. Chem.*, **87,** 151 (1991).
6. J. M. Ginder and L. C. Davis, *Appl. Phys. Lett.*, **65,** 3410 (1994).
7. C. Tan and T. B. Jones, *J. Appl. Phys.*, **73,** 3593 (1993).
8. T. Shiga, T. Ohta, Y. Hirose, A. Okada, and T. Kurauchi, *Koubunshi Ronbunshu*, **48,** 47 (1991).
9. T. Shiga, T. Ohta, Y. Hirose, A. Okada, and T. Kurauchi, *J. Mater. Sci.*, **28,** 1293 (1993).
10. T. Shiga, A. Okada, and T. Kurauchi, *J. Appl. Polym. Sci.*, **58,** 787 (1995).
11. T. Shiga, A. Okada, and T. Kurauchi, *Macromolecules*, **26,** 6958 (1993).
12. T. Shiga and A. Okada, *Polym. Prepr. Jpn.*, **43,** 1336 (1994).
13. K. Tamao, S. Komada, I. Nakajima, and M. Kumada, *Tetrahedron*, **38,** 3347 (1982).
14. M. Sato, S. Tanaka, and K. Kaeriyama, *J. Chem. Soc. Chem. Commun.*, 873 (1986).
15. K. Yoshino, S. Nakajima, and R. Sugimoto, *Jpn. J. Appl. Phys.*, **26,** L1038 (987).
16. J. Laakso, J. E. Osterholm, and P. Nyholm, *Syn. Met.*, **28,** C467 (1989).
17. Y. Wang and M. F. Rubner, *Syn. Met.*, **39,** 153 (1990).
18. M. J. Winokur, D. Spiegel, Y. Kim, S. Hotta, and A. J. Heeger, *Syn. Met.*, **28,** C419 (1989).
19. S. Cen, and J. Ni, *Macromolecules*, **25,** 6081 (1992).
20. K. Tashiro, K. Ono, Y. Minagawa, M. Kobayashi, T. Kawai, and K. Yoshino, *J. Polym. Sci. Phys.*, **29,** 1223 (1991).
21. M. J. Winokur, P. Wamsley, J. Moulton, P. Smith, and A. J. Heeger, *Macromolecules*, **24,** 3812 (1991).
22. T. A. Skothem, *Handbook of Conducting Polymers*, Marcel Dekker, New York, 1986.

Received March 4, 1996
Accepted April 16, 1996